

Multiresolutional piecewise-linear image decompositions:  
Quantization errors propagation and design of “stable” compression schemes\*

Oleg Kiselyov and Paul Fisher  
Department of Computer Science  
PO Box 13886  
University of North Texas  
Denton Texas 76203-3886

*Phone: (817) 565-2767, FAX: (817) 565-2799*  
*Email: oleg@ponder.csci.unt.edu, fisher@gab.unt.edu*

Index words: image compression, tile-effect-free image compression, lossy compression, multiresolutional analysis, subband image coding.

### **Abstract**

The paper introduces a new approach to design of stable tile-effect-free multiresolutional image compression schemes. Rather than discussing convergence and other formal mathematical properties of multiresolutional analysis, the paper focuses on how quantization errors in decomposition coefficients affect the quality of the decompressed picture, how the errors propagate in a multiresolutional decomposition, and how to design a compression scheme where the effect of quantization errors is minimized (visually and quantitatively). The paper also introduces and analyzes the simplest family of Laplacian pyramids which yield multiresolutional piecewise-linear image decompositions. The error propagation analysis presented in the paper has led to discovery of particular Laplacian pyramids where quantizations errors do not amplify as they propagate, but quickly decay. Examples are provided and extensions of the family of decompositions to give piecewise-quadratic approximations are discussed.

### **I. Subband image analysis and tile-effect in the reconstructed signal**

Separating image features according to their ‘scale’, that is, classifying them into appropriate resolution subbands, is equivalent to passing the image through a two-dimensional filter bank, a collection of filters where each filter passes only one particular ‘frequency/resolution band’ of image features and cuts off everything else [SIMO91, MALL89]. Each of the bands may be subsampled. One particular type of the subband decomposition exists when the separate filters in the bank are constructed according to a single rule:

---

\* This work supported in part by US Navy SPAWAR Grant N00039-94-C-0013 “Compression of Geophysical Data” and by US Army Research Office TN 93-461 administered by Battelle Research Office.

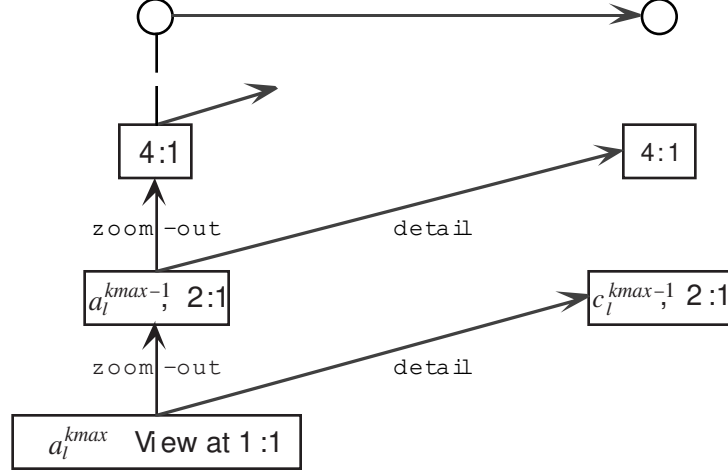


Fig. 1. Multiresolutional image analysis in its most general form of subband coding with iterated filter banks and subsampling of the high-pass band

The original signal (image) is at the very bottom of the left-hand side pyramid, a Gaussian pyramid [BURT83], which represents a set of views of the signal at different resolutions. Subsequent levels of the pyramid are constructed by successively applying a **zoom-out** operation

$$a_l^{k-1} = \sum_m g(2l-m) a_m^k, \quad l = 0..2^{k-1}-1, \quad m = 0..2^k-1 \quad (1)$$

which ‘averages out’ fine image details with low-pass filtration and performs a subsampling, thus reducing the resolution twice. The Laplacian pyramid [BURT83] is on the right-hand side of the picture. It is obtained by using a **detail** operation, which is similar to **zoom-out** but uses a complementary filter  $h(i)$  to isolate the high-frequency band  $c_l^k$ , which retains the features left out during the **zoom-out** operation:

$$c_l^{k-1} = \sum_m h(2l-m) a_m^k, \quad l = 0..2^{k-1}-1, \quad m = 0..2^k-1 \quad (2)$$

where  $h(i)$  is obviously a high-pass filter. Note that the detail band is also subsampled. The low-pass band  $a_l^{k-1}$  is treated in a similar way on the next step of the procedure, and split into the even lower resolution, and the detail components. Thus, recursive construction of the pyramid from the bottom to the top, Fig. 1, achieves the multiresolutional decomposition by separating the original signal into (octave) resolution bands  $c_l^k$  by applying a bank of iterated filters  $g$  and  $h$ . It can be shown that if the filters  $g$  and  $h$  are causal ones, then the original signal can always be reconstructed in its entirety by reversing the pyramid construction algorithm and merging the bands. Sections 2 and 3 below illustrate this point.

Again, the reconstruction in the absence of quantization errors is always perfect. However, to achieve high compression ratios, the decomposition coefficients have to be quantized, which inevitably leads to reconstruction errors. The most frequently occurring distortion is blockiness, or tile-effect. Errors of this type always arise when the high-pass filter has the following form:

$$c_l^{k-1} = a_{2l+1}^k - a_{2l}^k, \quad l = 0..2^{k-1}-1, \quad (3)$$

which is the filter used in the Haar wavelet decomposition [DEVO92, KIFI93]. Indeed, suppose we performed such a quantization of the wavelet decomposition that all bottom level coefficients  $c_l^{kmax-1}$  are set to 0 (a very common case). It immediately follows that the first derivative of the restored function would be zero on intervals  $[2l, 2l+1]$ , that is, the restored function would be piecewise-constant,  $a_{2l}^{kmax} = a_{2l+1}^{kmax}$ , with possible large breaks from  $a_{2l+1}^{kmax}$  to  $a_{2l+2}^{kmax}$ . That is exactly what blockiness means. Another easy way of looking at it is to decompose a sample ramp function  $f_i = h+i \cdot g$  and then set  $c_l^{kmax-1}$  to 0. In the original function,  $f(i+1)-f(i) = g$  is always constant. In the restored function,  $f(2i+1)-f(2i) = 0$ , but  $f(2i+2)-f(2i+1) = 2g$  (big step). It is interesting to note that no matter which low-pass filter is used, the blockiness would always exist as long as the high-pass filter, eq. (2), is of the first order. Thus, to avert blockiness, we need to use higher-order filters. The paper also shows that the way to avoid the tile-effect, in terms of the wavelet analysis, is to allow overlap in integer translates of the scaling function (mother wavelet)  $\phi(x)$ , which implies that  $\text{supp}[\phi(x)]$  should extend beyond  $[0,1]$ .

## II. 1D piecewise-linear stable multiresolutional decompositions

The present paper thoroughly analyzes the subband image coding with iterative filter banks in the simplest case of 3-point causal filters. For the sake of clarity, we consider one-dimensional signal decompositions first. As we saw above, the only way to eliminate the blockiness (piecewise constantness) upon quantizing of decomposition coefficients is to use a high-pass filter of the order higher than one. For example, if we employ a second-order filter, quantizing of decomposition coefficients results in a piecewise linear function, i.e., a function with a piecewise constant first derivative. This gives much better visual appearance than blockiness, as examples in the next two sections illustrate.

There is only one 3-point second-order high-pass causal filter (up to normalization):

$$c_i^{k-1} = a_{2i-1}^k - 2a_{2i}^k + a_{2i+1}^k \quad (4)$$

As to the low-pass filter, for a moment we consider it as general as a 3-point causal filter can be. Thus, we will analyze the following decomposition formulas:

$$a_i^{kmax} = f_i \text{ (original signal)} \quad (5_1)$$

$$c_i^{k-1} = a_{2i-1}^k - 2a_{2i}^k + a_{2i+1}^k, i > 0; \quad c_0^{k-1} = a_1^k - a_0^k \quad (5_2)$$

$$a_i^{k-1} = p_1 a_{2i-1}^k + p_2 a_{2i}^k + p_3 a_{2i+1}^k, \quad k > 0 \quad (5_3)$$

We consider  $a_{-1}^k \equiv a_0^k$ , assuming the signal continuity through the sample border. Eq. (5<sub>3</sub>) has to be a low-pass filter so that the constant signal can pass unharmed. In other words, if the signal does not change over the span of three sample points, it obviously represents a larger-scale feature (with no fine details), which should be passed over and dealt with at higher levels of the decomposition. Therefore, we have the following requirement for coefficients p<sub>1</sub>-p<sub>3</sub>:

$$p_1 + p_2 + p_3 = 1 \quad (6_1)$$

Moreover, we also want coefficients to satisfy the following “desirable” properties:

$$p_1 - p_2 + p_3 = 0 \quad (6_2)$$

$$p_2 > 0, \quad p_3 > 0 \quad (6_3)$$

Equation (6<sub>2</sub>) essentially says that the filter should cut off the highest possible frequency completely. It is easy to see that along with eq. (6<sub>1</sub>) it leads to p<sub>2</sub>=1/2. Though this is not a strict requirement, it is still a desirable property for a low-pass filter. The reconstruction formulas are:

$$a_0^{k+1} = (a_0^k - p_3 c_0^k) / (p_1 + p_2 + p_3), \quad (7_1)$$

$$a_1^{k+1} = (a_0^k + (p_1 + p_2) c_0^k) / (p_1 + p_2 + p_3), \quad (7_2)$$

$$a_{2i}^{k+1} = (a_i^k - p_3 c_i^k + (p_3 - p_1) a_{2i-1}^{k+1}) / (p_2 + 2p_3), \quad (7_3)$$

$$a_{2i+1}^{k+1} = (2a_i^k + p_2 c_i^k - (p_2 + 2p_1) a_{2i-1}^{k+1}) / (p_2 + 2p_3), \quad i > 0 \quad (7_4)$$

If both p<sub>2</sub> and p<sub>3</sub> are positive, then it is obvious that the formulas are stable with regard to a small error in c<sub>i</sub><sup>k</sup>. To keep the errors in a<sub>i</sub><sup>k</sup> and a<sub>2i-1</sub><sup>k+1</sup> from amplifying, we need the following conditions:

$$(p_3 - p_1) / (p_2 + 2p_3) < 1 \quad (8_1)$$

$$(p_2 + 2p_1) / (p_2 + 2p_3) < 1 \quad (8_2)$$

$$p_2 / (p_2 + 2p_3) < 1, \quad p_3 / (p_2 + 2p_3) < 1 \quad (8_3)$$

$$2 / (p_2 + 2p_3) < 1 \quad (8_4)$$

If both  $p_2$  and  $p_3$  are positive (as desired), then (8<sub>3</sub>) holds automatically. Eq. (8<sub>1</sub>) is also satisfied because of (6<sub>1</sub>). Eqs. (8<sub>2</sub>) and (8<sub>4</sub>) along with eq. (6<sub>1</sub>) give rise to the following stability condition:

$$p_3 > 1 + p_1 \quad (9)$$

Incidentally, it implies that  $p_1$  must be negative. Note, if we want to make  $p_2=p_3$ , we must have  $p_2=p_3>2/3$  and  $p_1<-1/3$ .

To see clearly what a difference a stable filter makes, consider the following three choices for the low-pass filter coefficients:

$$p_1 = 0, \quad p_2 = \frac{1}{2}, \quad p_3 = \frac{1}{2} \quad (10)$$

$$p_1 = -\frac{1}{4}, \quad p_2 = \frac{1}{2}, \quad p_3 = \frac{3}{4} \quad (11)$$

$$p_1 = -\frac{1}{4}, \quad p_2 = \frac{1}{4}, \quad p_3 = 1 \quad (12)$$

Eq. (10) corresponds to a very unstable filter, which lets quantization errors propagate with amplification; Eq.(11) is the borderline case, where the errors do not amplify, but do not decay in some cases either. Eq. (12) specifies the stable filter, where an error in a decomposition coefficient  $c_l^k$  quickly decays and does not significantly spread.

To get a better picture of distortions in the reconstructed signal due to the quantization of decomposition coefficients, we conducted some 1D simulations in MATLAB using various waveforms for the original signal, which can be considered a cross-section (profile) of a two-dimensional image. The present abstract shows a few sample results for a gaussian, that is, bell-shaped waveform. This waveform is a good realistic approximation for a profile of a sharp edge in a picture. In MATLAB notation, the waveform can be described as

$$\text{orig\_signal} = (255*\exp(-(x-16).^2/40)+10)$$

The original signal was decomposed into a number of subbands using formulas (7) with a low-pass filter specified by each of eqs. (10-12), in turn. The decomposition was quantized in such a way that three bottom level bands were completely leveled off (that is,  $c_l^k$  were set to zero for all  $l$  and  $k=kmax, kmax-1$ , and  $kmax-2$ ). The following pictures show the original signal (always in light gray) and the signal reconstructed after the quantization of the subband decomposition:

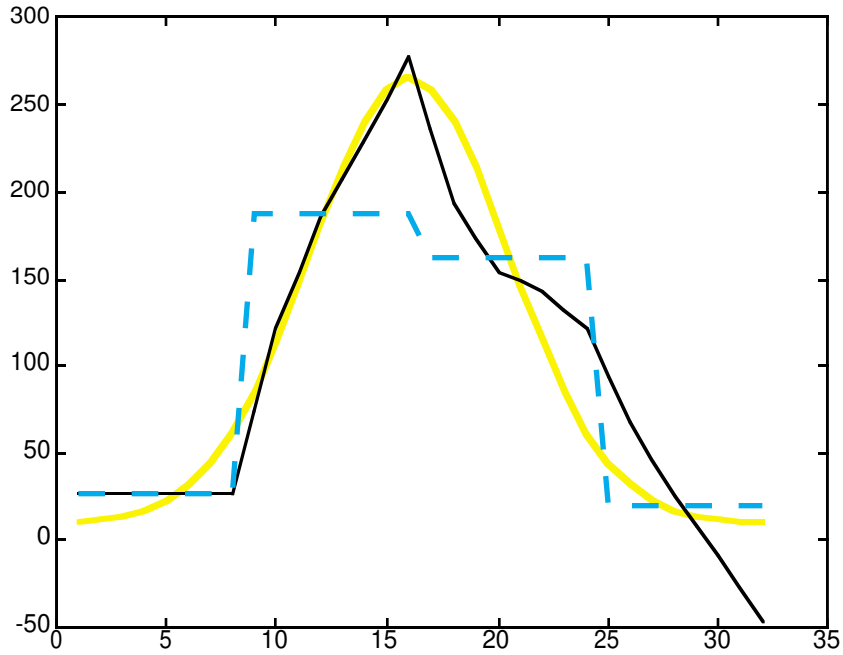


Fig. 2. Original “bell profile” and reconstructed one after the quantization with the low-pass filter (10). Maximum absolute reconstruction error is 60.42. Piecewise constant reconstruction is shown in dash line.

The figure clearly demonstrates that after three levels of the decomposition coefficients have been zeroed in, the reconstruction is rather poor: the ringing is quite noticeable and the edge is significantly blurred. This is a consequence of the “instability” of the decomposition, in the sense defined above. Fig. 2 also plots a result for the Haar-wavelet decomposition quantized to a comparable level. As one can see, even a far from perfect piecewise-linear reconstruction is still better than the piecewise-constant one.

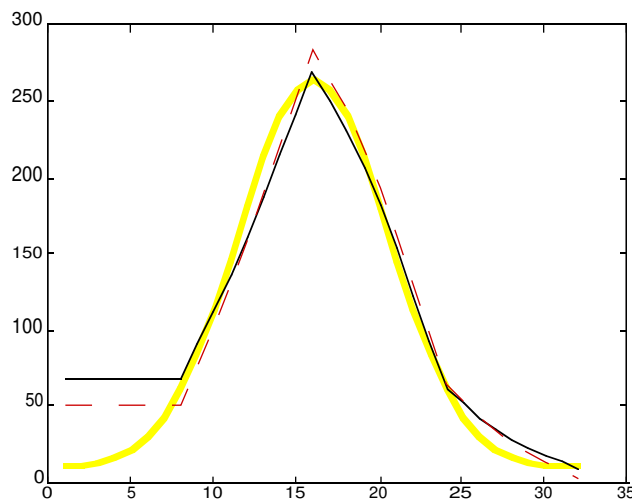


Fig. 3. Original “bell profile” and reconstructed ones after the quantization with the low-pass filters: eq. (11) (in gray dash) and eq. (12) (black solid). Maximum absolute reconstruction errors are 34.98 and 64.80, and  $\mathbf{L}_1$  errors 14.39 and 19.79, max of a derivative 29.50 and 35.19 correspondingly (max of a derivative for the original signal being 34.43)

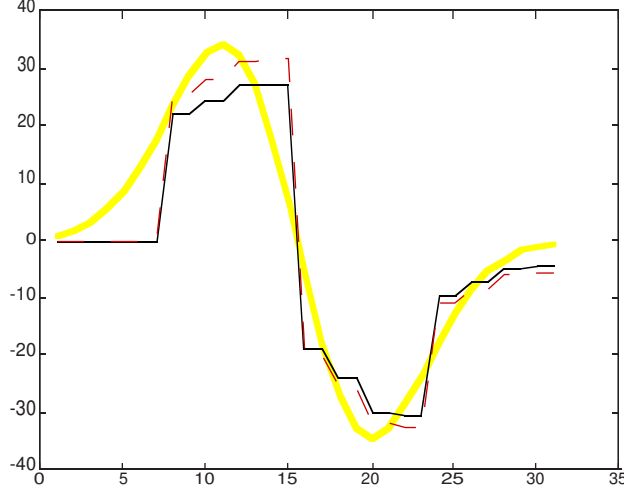


Fig. 4. First derivative of the original “bell profile” and the reconstructed signals after the quantization with the low-pass filters: eq. (11) (in gray dash) and eq. (12) (black solid)

Figures 3 and 4 show that a stable 3-point low-pass filter makes quite a difference. The plot of the first derivative on Fig. 4 points out very clearly that in spite of a harsh quantization, the reconstructed signal conveys rather accurately the form and shape of the original signal, asserting not only the tile-effect-free reconstruction but also a high contrast.

### III. Stable high-contrast image compression scheme

The present section generalizes the stable subband decomposition algorithm outlined above for images, two-dimensional signals. In the 2D case, we use separable filters, which are tensor products of the corresponding 1D functions. Note, that now we have one low-pass filter and three high-pass filters:

$$\begin{aligned}
 16a_{ij}^{k-1} &= a_{2i-1,2j-1}^k - a_{2i-1,2j}^k - 4a_{2i-1,2j+1}^k \\
 &\quad - a_{2i,2j-1}^k + a_{2i,2j}^k + 4a_{2i,2j+1}^k \\
 &\quad - 4a_{2i+1,2j-1}^k + 4a_{2i+1,2j}^k + 16a_{2i+1,2j+1}^k
 \end{aligned} \tag{13_1}$$

$$\begin{aligned}
 8cv_{ij}^{k-1} &= -a_{2i-1,2j-1}^k + a_{2i-1,2j}^k + 4a_{2i-1,2j+1}^k \\
 &\quad + 2a_{2i,2j-1}^k - 2a_{2i,2j}^k - 8a_{2i,2j+1}^k \\
 &\quad - a_{2i+1,2j-1}^k + a_{2i+1,2j}^k + 4a_{2i+1,2j+1}^k
 \end{aligned} \tag{13_2}$$

$$\begin{aligned}
8ch_{ij}^{k-1} &= -a_{2i-1,2j-1}^k + 2a_{2i-1,2j}^k - a_{2i-1,2j+1}^k \\
&+ a_{2i,2j-1}^k - 2a_{2i,2j}^k + a_{2i,2j+1}^k \\
&+ 4a_{2i+1,2j-1}^k - 8a_{2i+1,2j}^k + 4a_{2i+1,2j+1}^k
\end{aligned} \tag{133}$$

$$\begin{aligned}
4cd_{ij}^{k-1} &= a_{2i-1,2j-1}^k - 2a_{2i-1,2j}^k + a_{2i-1,2j+1}^k \\
&- 2a_{2i,2j-1}^k + 4a_{2i,2j}^k - 2a_{2i,2j+1}^k \\
&+ a_{2i+1,2j-1}^k - 2a_{2i+1,2j}^k + a_{2i+1,2j+1}^k
\end{aligned} \tag{134}$$

Here  $ch$  band characterizes horizontal features,  $cv$  represents vertical ones, while  $cd$  band is related to diagonal image features [MALL89].

The paper talks at great length about how to perform decomposition so that all the coefficients are integral. It should be stressed that the reconstruction in absence of quantization is always perfect. The paper also tests the stable image compression method on a set of “standard” images, to show how well simple patterns of vertical/diagonal edges, ramp gradient fills, etc., are reconstructed. Since the patterns are very simple, it is easy to see what kind of visual distortion (blurring of an edge, ringing, lost contrast, staircase diagonal edge, etc.) a particular compression technique introduces. Moreover, however simple the patterns are, they represent most characteristic and most common (tiny) parts of a complex picture. Therefore, if reconstruction of the simple images appears pleasant, one can expect good results for realistic images, too. Given below is an example for one of the simple test patterns:



Fig. 5a. Original test pattern



Fig. 5b. reconstructed pattern after ripping off three bottom layers, RMSE 17.90,  $L_1$  error 7.80,  $L_\infty$  error 94



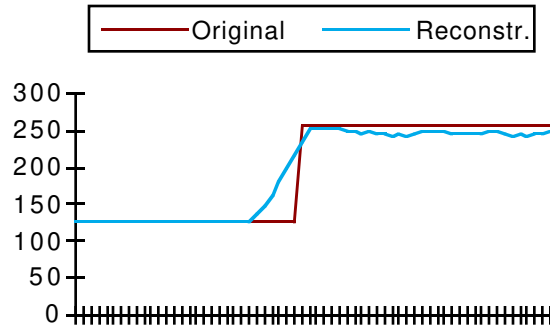


Fig. 5c. Horizontal cross-section of the patterns, Figs. 5a and 5b.

Finally, the following pictures show how well the proposed subband coding algorithm works for “real” images, a satellite picture of clouds in particular:

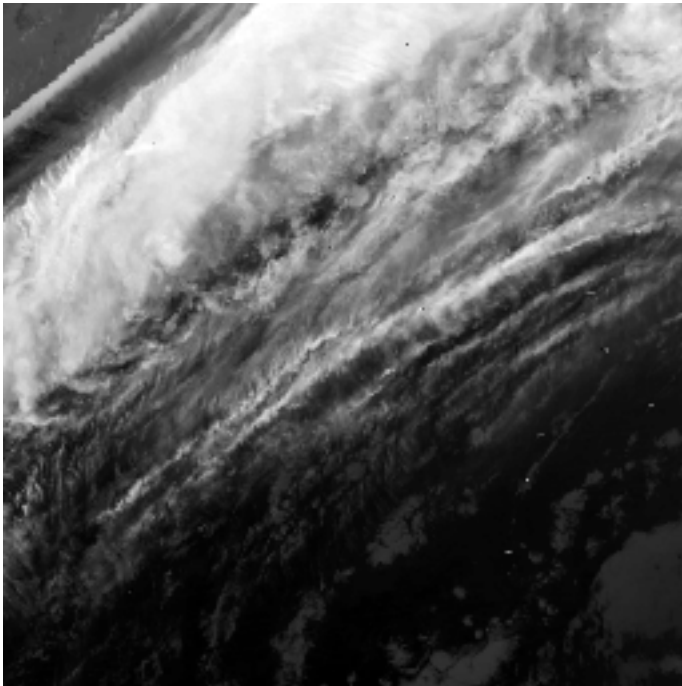


Fig. 6a. Original Clouds. Printed at scale 2:1 after the contrast enhancement of the inverted LUT.

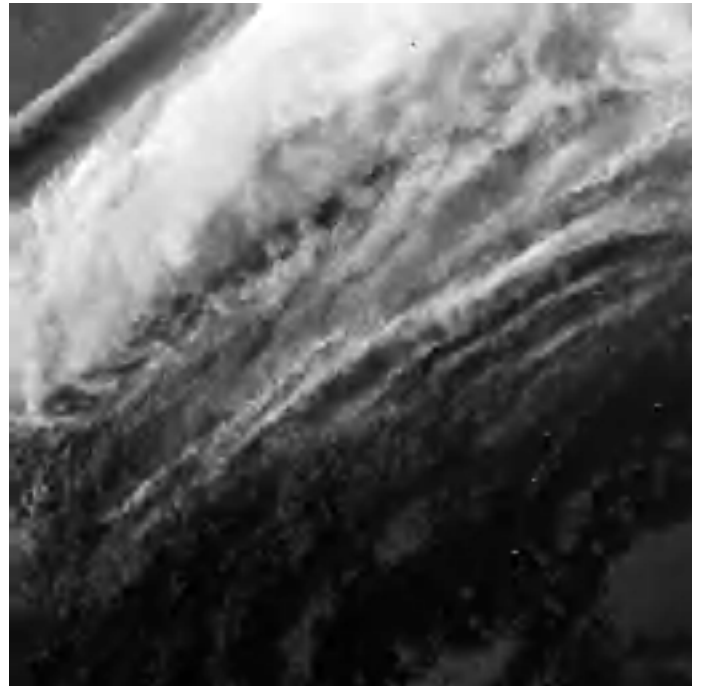


Fig. 6b. Compressed image, compression ratio 40:1, RMSE 6.26,  $L_1$  error 4.22

The reconstructed picture does not look blocky at all, even at relatively high compression ratios: usually when the ratio reaches 30:1, one can notice blockiness in the background of the picture if one uses JPEG or Haar-base wavelet compression.

## References

[BURT83] Burt, P., Adelson, E., “The Laplacian Pyramid as a Compact Image Code,” *IEEE Trans. Comm.*, Vol. 31, No. 4, pp. 532-540, April 1983.

[DEVO92] DeVore, R. A., B. Jawerth, B. J. Lucier, "Image Compression Through Wavelet Transform Coding," *IEEE Trans. Inf. Theory*, Vol. 38, No. 2, pp. 719-746, 1992.

[KIFI93] Kiselyov, O. and P. Fisher, "Pyramidal Image Decompositions: A New Look," in *Proc. DCC'93, 1993 Data Compression Conference*, Snowbird, Utah, p.479, March 30-April 2, 1993.

[MALL89] Mallat S., "A Theory for Multiresolutional Signal Decomposition: the Wavelet Representation," *IEEE Trans. on Pattern Analysis and Machine Intell.*, Vol. 11, No. 7, pp.674-693, July 1989.

[SIMO91] Simoncelli E.P., Adelson E.H., "Subband Transforms," in *Subband Image Coding*, Ed. J.W.Woods, Chapter 4, Kluwer Academic Publishers, 1991.